Light scattering by Landau levels driven by intense terahertz radiation

Takeshi Inoshita*
Quantum Transition Project, ICORP, JST, 4-1-8 Honcho, Kawaguchi, Saitama 332-0012, Japan
(Received 17 March 1999)

An analytic theory of near-infrared (NIR) light scattering (sideband generation) by an undoped quantum well subjected to intense terahertz radiation and a quantizing magnetic field is presented. The response of Landau-quantized carriers (created by the NIR light) to the terahertz field is singular at cyclotron resonance due to the characteristic energy structure of the Landau levels. These singularities, absent in the conventional optical Stark effect of atoms, manifest themselves as disappearance of sidebands at resonance or in the limit of strong terahertz intensity.

Discrete electronic systems, e.g., atoms, usually have a distribution of energy-level spacings. In discussing the interaction of such systems with intense monochromatic radiation (optical Stark effect), it is permissible to single out a few pairs of levels that are close to resonance and neglect all others. The interaction merely renormalizes the level energies and other dynamic quantities (e.g., velocity) by a finite amount and no singularity arises even at resonance.[1] This simplified *dressed-atom* picture fails for Landau-quantized electrons in a parabolic band. There being an infinite number of equally spaced levels, it is necessary to treat the whole ladder of levels on an equal footing. In this paper, we will first show that, in the absence of level broadening, the dynamic response of Landau levels (LL's) to an ac electric field *diverges* at resonance due to their characteristic energy structure. We then argue that this singularity drastically alters the scattering of light (weak probe beam) by ac-driven LL's. This is substantiated by a numerical calculation that takes into account LL broadening.

In discussing light scattering, we specifically investigate the setup used in the recent experiment by Kono and co-workers[2–6] who examined the scattering of weak near-infrared (NIR), near-band-gap, radiation (frequency Ω) in GaAs quantum wells subjected to a strong magnetic field and driven by intense terahertz (THz) radiation (frequency ω) generated by a free-electron laser. (In GaAs, the electron cyclotron frequency is in the terahertz range for magnetic fields >2 T.) Aside from usual photoluminescence, sharp emission lines, or sidebands, were observed at $\Omega+2n\omega$ ($n=\pm1,+2$). We formulate an analytic theory for these sidebands taking into account the THz field nonperturbatively while treating the NIR field in the first order. A remarkable finding is the disappearance of the sidebands for sufficiently large THz intensity or very close to a cyclotron resonance (CR), which is a consequence of the aforementioned singularity.[7]

So far, experiments have shown no evidence of such singularity [2–6] and they can be described adequately by a perturbation theory that assumes the weakness of both THz and NIR fields.[8,9] Since the novel phenomena predicted are nonperturbative effects, their observation would require a THz source of stronger (but not unrealistically strong) intensity or a sample of higher quality.

Let us consider an undoped GaAs multiple quantum-well structure at $T=0$ (growth axis $\|z$) in a quantizing magnetic field $\boldsymbol{B}=(0,0,B)$ irradiated simultaneously by THz and NIR radiation, both polarized linearly in the well plane (Fig. 1). The barrier layers are sufficiently thick that the wave functions of different wells do not overlap with each other. The sample is taken to be rectangular with side lengths L_x and L_y. We adopt a simple two-band parabolic approximation, taking into account the lowest conduction subband and the highest valence subband, with in-plane effective mass $m_c>0$ and $-m_v<0$, respectively. Electron-electron and electron-hole interactions are neglected altogether. [The latter approximation is valid if $eB/\mu c \gg \mu e^4/2\kappa^2$, where $\mu=(m_c^{-1}+m_v^{-1})^{-1}$ is the reduced mass, c the light velocity in vacuum, κ the static dielectric constant, and we put $\hbar=1$. For GaAs, this condition is satisfied if $B \gg 1$ T.]

Assuming that the THz field is not so strong as to mix the two bands and disregarding the NIR field for the moment, the two bands can be treated separately. Writing the THz electric field as $(E_{\mathrm{THz}}\sin\omega t,0,0)$ and choosing the vector potential as $\boldsymbol{A}=(0,Bx,0)$, the envelope functions ψ^c for the conduction band (CB) electrons, with charge $-e<0$, driven by the THz field can be obtained by solving the effective-mass equation $H\psi^c=i\partial\psi^c/\partial t$ with the Hamiltonian[10]

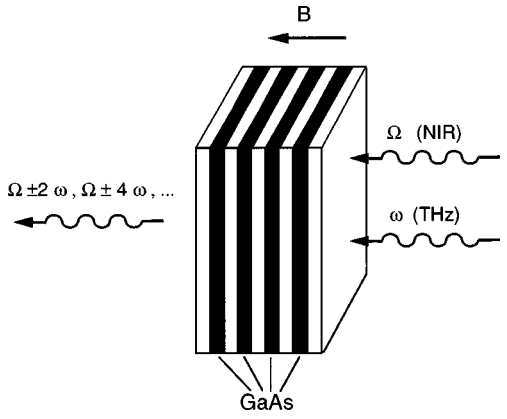

FIG. 1. Schematic of the light-scattering setup studied. The magnetic field and the wave vectors of the light beams (NIR and THz) are all perpendicular to the well plane.

 ©2000 The American Physical Society

$$H=\frac{1}{2m_c}\left(-\frac{\partial^2}{\partial x^2}-\frac{\partial^2}{\partial y^2}-\frac{2ieBx}{c}\frac{\partial}{\partial y}+\frac{e^2B^2}{c^2}x^2\right)+eE_{\mathrm{THz}}x\sin(\omega t). \quad (1)$$

Now, we set $\psi^c(x,y,t)=L_y^{-1/2}\exp[-ieBXy/c+ieE_{\mathrm{THz}}X\cos(\omega t)/\omega]\phi^c(x-X,t)$ where $X=-cp_y/eB$ with $\boldsymbol{p}=(p_x,p_y,p_z)$ denoting the electron momentum. $\phi^c(x,t)$ can be shown to satisfy the Schrödinger equation for a driven harmonic oscillator. The stationary solutions of this equation read[11]

$$\phi^c(x,t)=\chi_n^c(x-\gamma_c)\exp\left(-iE_n^ct+im_c\dot{\gamma}_c(x-\gamma_c)+i\int^t L_c(s)ds\right). \quad (2)$$

Here $\chi_n^c(x)$ is the nth harmonic oscillator eigenfunction with energy $E_n^c=\omega_{0c}(n+1/2)$ $(n=0,1,2,\ldots)$, $\omega_{0c}=eB/m_cc$ is the CB cyclotron frequency, $\gamma_c(t)=eE_{\mathrm{THz}}\sin(\omega t)/m_c(\omega^2-\omega_{0c}^2)$ is a classical trajectory, $L_c(t)=m_c\dot{\gamma}_c^2/2-m_c\omega_{0c}^2\gamma_c^2/2-eE_{\mathrm{THz}}\gamma_c\sin(\omega t)$ is the Lagrangian for $\gamma_c(t)$, and $\dot{\gamma}_c=d\gamma_c/dt$. Combining all these, we get

$$\psi_{nX}^c(x,y,t)=\frac{1}{\sqrt{L_y}}\chi_n^c(x-X-\gamma_c)e^{-i\bar{E}_n^ct-iXy/\ell^2+iG_c}, \quad (3)$$

with

$$G_c(t)=g_{c1}\cos(\omega t)+g_{c2}\sin(2\omega t), \quad (4a)$$

$$\bar{E}_n^c=\left(n+\frac{1}{2}\right)\omega_{0c}+\frac{e^2E_{\mathrm{THz}}^2}{4m_c(\omega^2-\omega_{0c}^2)}, \quad (4b)$$

where $n=0,1,2,\ldots$, $\ell=\sqrt{c/Be}$ is the magnetic length, and $g_{c1,2}$ are functions of ω, B, E_{THz}, x, and X.

If $E_{\mathrm{THz}}=0$, it is well known that the eigenfunctions of H can be designated by the quantum numbers n (Landau index) and X (cyclotron center coordinate).[12] Equations (3) and (4) show that even when $E_{\mathrm{THz}}\neq 0$, the stationary solutions can be designated by the same parameters n and X. The electron undergoes a cyclotron motion with frequency ω_{0c} around the *moving* center whose x coordinate is $\bar{X}(t)\equiv X+\gamma_c(t)$. Note that $\bar{X}(t)=X$ at $t=(2\pi/\omega)n$ $(n=0,\pm1,\pm2,\ldots)$. In the classical limit, the cyclotron center revolves along an elliptic orbit with frequency ω and radii $\propto E_{\mathrm{THz}}/|\omega^2-\omega_{0c}^2|$.

It is seen from Eqs. (3) and (4) that $\psi_{nX}^c(x,y,t)$ has temporal Fourier components $\bar{E}_n^c\pm n\omega$ $(n=0,1,2\ldots)$, i.e., the LL's split into THz side levels. Furthermore, the THz field shifts these levels uniformly by $e^2E_{\mathrm{THz}}^2/4m_c(\omega^2-\omega_{0c})^2$. Namely, the level energies diverge at CR while the level separation is kept unchanged at the unperturbed value ω_{0c}. Other dynamic quantities, e.g., velocity, diverge as well. This behavior is totally different from the usual dynamic Stark effect, where these quantities are dressed without any singularity.

As for the *valence band* (VB), the solutions are obtained by simply replacing m_c by $-m_v$ in Eqs. (3) and (4). Let us denote the VB counterparts of $\psi_{nX}^c(x,t)$, ω_{0c}, $\gamma_c(t)$, and $\bar{E}_n^c$ by $\psi_{nX}^v(x,t)$, ω_{0v}, $\gamma_v(t)$, and $\bar{E}_n^v$, respectively.[13]

Now, let us introduce the NIR field, which couples the CB and VB, in the lowest order. This requires the use of the full wave functions, including the Bloch parts, instead of the envelope functions. Tildes will be used to denote the full wave functions, i.e., $\tilde{\psi}_{nX}^c(xt)$ is the product of $\psi_{nX}^c(xt)$ and the CB Bloch function at the Brillouin zone center. Starting from $\tilde{\psi}_{nX}^v(x,t)$ at $t=t_0$ (long past), and turning on the NIR field $\boldsymbol{E}_{NIR}$ slowly with the interaction $H_{NIR}(t)=-ie\boldsymbol{E}_{NIR}(t)\cdot\boldsymbol{p}/m_0\Omega$ (m_0 is the bare electron mass), the wave function at $t\gg t_0$, to first order in H_{NIR}, can be written as $\tilde{\psi}_{nX}^v+\delta\tilde{\psi}_{nX}$ with

$$\delta\tilde{\psi}_{nX}(t)=-i\sum_{n'X'}\tilde{\psi}_{n'X'}^c(t)\lim_{t_0\to-\infty}\int_{t_0}^t ds\langle\tilde{\psi}_{n'X'}^c(s)\times|H_{NIR}(s)|\tilde{\psi}_{nX}^v(s)\rangle e^{\epsilon s}, \quad (5)$$

where $e^{\epsilon s}$ ($\epsilon>0$ is a small number) was inserted to ensure slow switching of the NIR field. To discuss NIR light emission, we need the interband current

$$\boldsymbol{j}(t)=-\frac{2eN}{m_0}\sum_{nX}\langle\tilde{\psi}_{nX}^v(t)+\delta\tilde{\psi}_{nX}(t)|\boldsymbol{p}|\tilde{\psi}_{nX}^v(t)+\delta\tilde{\psi}_{nX}(t)\rangle, \quad (6a)$$

$$=-\frac{2eN}{m_0}\sum_{nX}\langle\tilde{\psi}_{nX}^v(t)|\boldsymbol{p}|\delta\tilde{\psi}_{nX}(t)\rangle+\text{c.c.}, \quad (6b)$$

where N is the number of wells per unit thickness and the factor 2 accounts for spin. Since $\boldsymbol{j}$ is parallel to $\boldsymbol{E}_{NIR}$ and isotropic in the layer plane, it suffices to set $\boldsymbol{E}_{NIR}=(E_{NIR}\sin\Omega t,0,0)$ and calculate $j\equiv j_x$.

In deriving Eqs. (5) and (6), we assumed that the electrons and holes created by the NIR field are described by the *stationary* wave functions $\tilde{\psi}_{nX}^c(t)$ and $\tilde{\psi}_{n'X}^v(t)$, respectively. This condition, together with the slow switching of the NIR field, limits our theory to stationary scattering, precluding any transient effects that might arise from the sudden application of the THz field.

To evaluate Eq. (6b) using Eq. (5), we need the matrix elements of p_x between $\tilde{\psi}_{n'X'}^c$ and $\tilde{\psi}_{nX}^v$:

$$\langle\tilde{\psi}_{nX}^c|p_x|\tilde{\psi}_{n'X'}^v\rangle=\delta_{XX'}Pe^{i(\bar{E}_n^c-\bar{E}_{n'}^v)t}\sum_{l=-\infty}^{\infty'}D(l,n,n')e^{-il\omega t}, \quad (7)$$

where P is the bulk interband matrix element of momentum,[14] the prime over the summation denotes that l runs over even (odd) integers if $(n-n')$ is even (odd), and $D(l,n,n')$ is an analytic function of ω, B and E_{THz}. Combining Eqs. (5)–(7), we obtain

$$j(t)=\frac{1}{2\pi}\sum_{n=-\infty}^{\infty}j_ne^{-i(\Omega+2n\omega)t}, \quad (8)$$

with

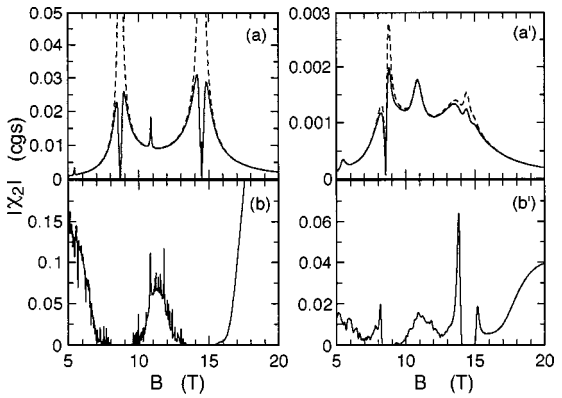

FIG. 2. $|\chi_{n=2}|$ vs B calculated for (a) $E_{\mathrm{THz}}=1$ and (b) 20 kV/cm with broadening parameters $\delta=\epsilon=0.1$ meV. At each E_{THz}, Ω is tuned to the Ω_{110} resonance, while ω is kept constant at 15 meV. Similar results calculated for larger broadening $\delta=\epsilon=1$ meV are presented in (a′) and (b′). In (a) and (a′), the results obtained by setting $e^{-\Lambda}=1$ are plotted by dashed lines. Throughout the paper, the following parameters are used for numerical calculations: $m_c/m_0=0.067$, $m_v/m_0=0.11$, $N=4\times10^5$ cm^{-1}, and $P=1.29\times10^{-19}$ g cm/s.

$$j_n=\frac{Ne^3E_{NIR}BP^2}{2cm_0^2\Omega}\sum_{l=0}^{\infty}\sum_{l'=0}^{\infty}\sum_{r=-\infty}^{\infty'}\times\frac{D(r+2n,l',l)D^*(r,l',l)}{\overline{E_l^c}-\overline{E_{l'}^v}+E_G-\Omega-(r+2n)\omega-i\epsilon},\qquad(9)$$

where E_G is the bulk band gap. Note that only even-order sidebands $\Omega\pm2n\omega$ appear and that j_n is resonantly enhanced when $\Omega=\Omega_{ii'q}\equiv\overline{E_i^c}-\overline{E_{i'}^v}+q\omega+E_G$, where q is an even (odd) integer if $i-i'$ is even (odd). ($\Omega_{ii'q}$ can be experimentally obtained from interband absorption spectra.)

In real systems, we expect the divergence at CR [as seen, e.g., in Eq. (4b)] to be suppressed by level broadening. To take account of finite LL width δ in the relaxation time approximation, we replace $\gamma_i(t)$ $(i=c,v)$ by a (classical) trajectory of a *damped* harmonic oscillator: $(eE_{\mathrm{THz}}/m_c)\sin(\omega t+\phi)/[(\omega^2-\omega_{0c}^2)^2+\delta^2\omega^2]$ where $\phi=\arctan[\delta\omega/(\omega^2-\omega_{0c}^2)]$. Inserting this into Eq. (2) and proceeding as before, we obtain modified expressions for Eqs. (4): $G_c(t)=g_{c1}'\cos(\omega t)+g_{c2}'\sin(2\omega t)+g_{c3}\cos(2\omega t)$ and $\overline{E_n^c}=(n+1/2)\omega_{0c}+(e^2E_{\mathrm{THz}}^2/4m_c)(\omega^2-\omega_{0c}^2)/[(\omega^2-\omega_{0c}^2)^2+\delta^2\omega^2]$. Although the final expression for $D(l,n,n')$ is complicated, we note, for later convenience, that at CR and for small δ,

$$D(l,n,n')\sim\exp\left(\frac{-E_{\mathrm{THz}}^2/2}{4\delta^2}\right)\equiv e^{-\Lambda}.\qquad(10)$$

We evaluate Eq. (9) using these generalized expressions. Since $j_n\propto E_{NIR}$, we define χ_n by $j_n=-i\omega\chi_nE_{NIR}$ and give our numerical results in terms of χ_n.[15]

The solid lines in Figs. 2(a) and 2(b) present the B dependence of $|\chi_{n=2}|$ calculated with level width $\delta=\epsilon=0.1$ meV for (a) $E_{\mathrm{THz}}=1$ and (b) 20 keV. Ω is tuned to the Ω_{110} resonance and ω is kept constant at 15 meV. In the weak-field case (a), there are two main resonances located near $B=8.7$ T and 14.4 T, which correspond to electron ($\omega=\omega_{0c}$) and hole ($\omega=\omega_{0v}$) CR's, respectively. The occurrence of CR peaks is consistent with our perturbation calculation.[8,9] A feature of our nonperturbative approach is the emergence of sharp downward cusps at the centers of the CR peaks. This phenomenon arises from the factor $e^{-\Lambda}$ in Eq. (10). (This is understood by comparing the solid line with the dashed line, which is obtained by replacing $e^{-\Lambda}$ by unity. Note the absence of any cusp in the latter.) The explanation is as follows: The recombination of an electron with a hole is possible only when they share the same X [Eq. (7)]. Hence the distance between the x components of their cyclotron centers is $|[X+\gamma_c(t)]-[X+\gamma_v(t)]|=|\gamma_c(t)-\gamma_v(t)|$, which increases resonantly as $\omega\to\omega_{0c}$ or ω_{0v}. (For $\delta=0$, it diverges in this limit.) This resonant electron-hole separation (REHS) causes the exponential decay (10) of the recombination probability and hence of sideband intensities. As E_{THz} increases, the cusps broaden and evolve into gaps, suppressing completely the CR peaks [Fig. 2(b)].

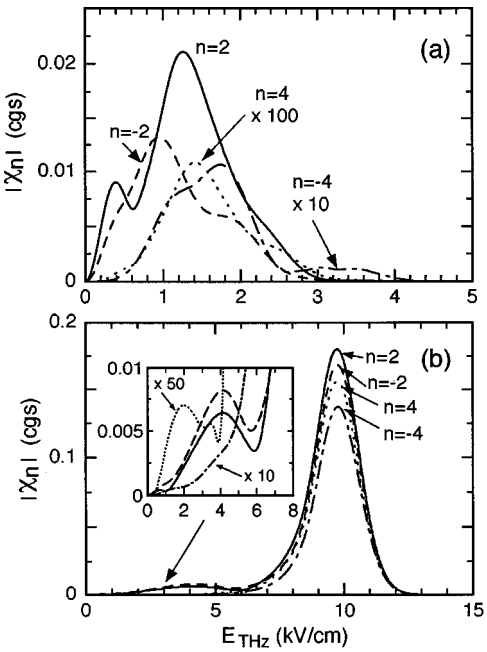

FIG. 3. Calculated $|\chi_n|$ vs E_{THz} for various sidebands n at $\omega=15$ meV. (a) and (b) correspond to $\delta=\epsilon=0.1$ and 1 meV, respectively. At each E_{THz}, Ω is tuned to the Ω_{220} resonance.

In Fig. 2(a), there is also a smaller peak at 10.9 T corresponding to $\omega=(\omega_{0c}+\omega_{0v})/2$. This peak, together with the one at 5.4 T, results from the denominator of Eq. (9). It is, therefore, unaffected by REHS and exhibits no cusp. As noted earlier, the denominator of Eq. (9) gives a number of resonances, of which only the one at $(\omega_{0c}+\omega_{0v})/2$ is dominant at small E_{THz}. As E_{THz} increases [Fig. 2(b)], more terms under the summation in Eq. (9) start to contribute with comparable weight, generating fine structures.

Figure 2(a′) presents the result for $E_{\mathrm{THz}}=1$ kV/cm calculated for larger level width $\delta=\epsilon=1$ meV with (solid line) and without (dashed line) the REHS factor $e^{-\Lambda}$. The two lines are quite similar, indicating that REHS is almost negligible compared to the smaller broadening case [Fig. 2(a)]. (The sharp drop near the center of the electron CR peak is not due to REHS.[16]) This is consistent with Eq. (10): level broadening weakens REHS. To observe REHS-induced ef-

fects at this broadening, we need larger THz intensity. Figure 2(b′), obtained for $E_{\mathrm{THz}}=20$ keV, shows clear REHS-induced gaps near CR. [The gaps are, of course, narrower than in Fig. 2(b).]

Figure 3(a) plots the E_{THz} dependence of $|\chi_n|$ ($n=\pm 2, \pm 4$) calculated for $B=8$ T, $\omega=15$ meV, $\Omega=\Omega_{220}$ (at each E_{THz}), and $\delta=\epsilon=0.1$ meV. Note that ω is chosen close to $\omega_{0c}=13.8$ meV. It is seen that $|\chi_n|$, which initially rises as $(E_{\mathrm{THz}})^n$, in agreement with the perturbation theory,[8,9] soon saturates and starts to oscillate. Eventually for $E_{\mathrm{THz}}>3$ keV, all the $|\chi_n|$ decay exponentially to zero. This decay is also due to the factor $e^{-\Lambda}$, i.e., REHS. It can be shown that the threshold THz intensity at which χ decays is roughly proportional to $\sqrt{(\omega-\omega_{0c})^4+\delta^2\omega_{0c}^2}$ (near electron CR). Thus, the sidebands persist up to higher E_{THz} if the detuning or δ is large. This THz-induced REHS also explains the oscillation of χ at intermediate E_{THz}. The recombining electron and hole, revolving along different trajectories, sense THz fields of different phases. This allows THz photons to be absorbed or emitted during recombination. Therefore, it is no coincidence that Fig. 3(a) resembles the current-voltage characteristics of photon-assisted tunneling in multiple quantum wells.[17]

Figure 3(b) presents similar results calculated for larger broadening $\delta=\epsilon=1$ meV. The larger threshold intensity (≈ 12 keV) is consistent with what was stated above. Immediately to the left of the threshold is a large peak whose shape is nearly independent of n. This peak results from LL broadening and is higher for larger δ. The oscillations are still clearly visible (inset) in the low-field regime. They eventually disappear as δ increases further.

In conclusion, we have theoretically discussed NIR sideband generation in an undoped semiconductor quantum well subject to intense THz radiation in quantizing magnetic fields. When the THz frequency is close to a CR, it drives the recombining electron and hole, created by the NIR light, away from each other and reduces their recombination probability. This resonant electron-hole separation causes the sideband intensity to oscillate as a function of E_{THz} and decay exponentially to zero as $E_{\mathrm{THz}}\rightarrow\infty$. The CR peaks exhibit a sharp downward cusp at their centers, which broaden as $E_{\mathrm{THz}}\rightarrow\infty$. Although the predicted effects are weakened by level broadening, they should still be observable in, e.g., GaAs quantum wells if the level width ~ 1 meV.

The author would like to thank J. Kono, T. Ando, H. Sakaki, M. S. Sherwin, and S. J. Allen, Jr. for illuminating discussions.

*Present address: Mesoscopic Correlation Project, JST, NTT Atsugi R&D Center 4S-308S, 3-1 Morinosato Wakamiya, Atsugi, 243-0198, Japan.

[1] See, for example, C. Cohen-Tannoudji, J. Dupont-Roc, and G. Grynberg, *Atom-Photon Interactions* (Wiley, New York, 1992), Chap. 6.

[2] J. Kono, M.Y. Su, T. Inoshita, T. Noda, M.S. Sherwin, S.J. Allen, Jr., and H. Sakaki, Phys. Rev. Lett. **79**, 1758 (1997).

[3] J. Černe, J. Kono, T. Inoshita, M.S. Sherwin, M. Sundaram, and A.C. Gossard, Appl. Phys. Lett. **70**, 3543 (1997).

[4] J. Kono, J. Černe, T. Inoshita, M.S. Sherwin, M. Sundaram, and A.C. Gossard, in *Proceedings of the 23rd International Conference on the Physics of Semiconductors*, edited by M. Scheffler and R. Zimmermann (World Scientific, Singapore, 1996), p. 1911.

[5] J. Kono, T. Inoshita, H. Sakaki, J. Černe, M.S. Sherwin, M. Sundaram, and A.C. Gossard, in *High Magnetic Fields in the Physics of Semiconductors II*, edited by G. Landwehr and W. Ossau (World Scientific, Singapore, 1997), p. 785.

[6] J. Kono, M.Y. Su, K.B. Nordstrom, J. Černe, M.S. Sherwin, S.J. Allen, Jr., T. Noda, T. Inoshita, and H. Sakaki, Proc. SPIE **3153**, 96 (1997).

[7] T. Inoshita and H. Sakaki, in *Proceedings.of the 24th International Conference on the Physics of Semiconductors*, edited by D. Gershoni (World Scientific, Singapore, 1999), CD-ROM 0085.pdf. Due to a numerical error in the prefactor, χ obtained in this paper should be multiplied by $(2\pi)^4$.

[8] T. Inoshita, J. Kono, and H. Sakaki, Phys. Rev. B **57**, 4604 (1998).

[9] T. Inoshita and H. Sakaki, Physica B **249-251**, 534 (1998).

[10] This problem was also treated in P. Hawrylak and L. Rego, Physica E (Amsterdam) **3**, 198 (1998). These authors obtained the time evolution operator instead of the wave functions.

[11] P. Hänggi, *Quantum Transport and Dissipation* (Wiley-VCH, Weinheim, 1998), Chap. 5.

[12] See, for example, H. Aoki and H. Kamimura, *The Physics of Interacting Electrons in Disordered Systems* (Oxford University, Oxford, 1989), Chap. 10.

[13] The field shifts $\bar{E}_n^c$ and $\bar{E}_n^v$ by different amounts, so the interband absorption energy depends on the THz field. This will be discussed in our forthcoming publication.

[14] P.Y. Yu and M. Cardona, *Fundamentals of Semiconductors* (Springer-Verlag, Berlin, 1996), p. 66.

[15] Since $j(t)/(-i\omega)$ is the polarization, χ denotes the ratio of the polarization to E_{NIR}.

[16] This drop results from the interference between the various terms under the summation in Eq. (9). Unlike the REHS-induced structures, such interference-induced structures are quite sensitive to the parameters and may occur at any value of B.

[17] For a review, see S.J. Allen, U. Bhattacharya, K. Campman, H. Drexler, A. Gossard, B.J. Keay, K. Maranowski, G. Medeiros-Ribero, M. Rodwell, J.S. Scott, C. Unterrainer, M. Wanke, and S. Zeuner, Physica B **227**, 367 (1996).